Joule

CellPress

Article

Storage and Recycling of Interfacial Solar Steam Enthalpy

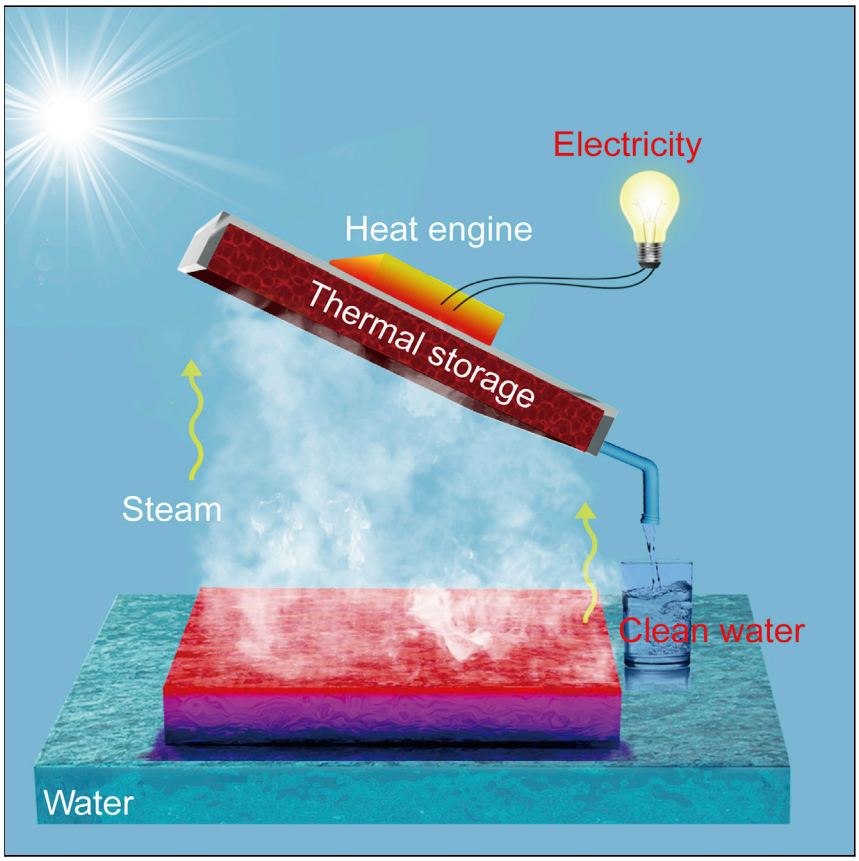

By using solar energy and sea (or contaminated) water, abundant resources on Earth, this solar device can generate clean water and electricity simultaneously, through storing and recycling the steam enthalpy derived from the interfacial solar steam-generation process. In addition, the integrated capability of thermal storage can enable electricity generation over an extended period after sunset. Combining conversion, storage, and utilization, this integrated solar energy device can provide the basic needs in various off-grid and/or resource-constrained areas.

Xiuqiang Li, Xinzhe Min, Jinlei Li, ..., Bin Zhu, Shining Zhu, Jia Zhu

jiazhu@nju.edu.cn

HIGHLIGHTS

Steam enthalpy is stored and recycled from interfacial solar steam process

This solar device can produce water and electricity simultaneously

The integrated thermal storage enables power generation after sunset

This integrated system combines solar energy conversion, storage, and utilization

Li et al., Joule 2, 1–8
November 21, 2018
https://doi.org/10.1016/j.joule.2018.08.008

Please cite this article in press as: Li et al., Storage and Recycling of Interfacial Solar Steam Enthalpy, Joule (2018), https://doi.org/10.1016/j.joule.2018.08.008

Joule

CellPress

Article

Storage and Recycling of Interfacial Solar Steam Enthalpy

Xiuqiang Li,[1,2] Xinzhe Min,[1,2] Jinlei Li,[1] Ning Xu,[1] Pengchen Zhu,[1] Bin Zhu,[1] Shining Zhu,[1] and Jia Zhu[1,3,*]

SUMMARY

In this work, it is shown that by storing and recycling steam enthalpy derived from the solar steam process, we can enable simultaneous generation of clean water and electricity. Energy-transfer efficiency of solar to steam can reach 72.2% with extra electricity power (with 1.23% efficiency) generated simultaneously. With advanced thermal management to further elevate the working temperature and exciting progress in the fields of thermoelectrics and desalination, it is expected that the performance of this system can be further improved. This approach with scalable materials and processes, high energy-transfer efficiency, and integrated storage capability will provide an attractive avenue to produce electricity and clean water in an individualized manner, particularly desirable in various off-grid areas.

INTRODUCTION

Clean water and electricity, essential to the daily life of humans, are unfortunately scarce resources in various parts of the world, especially in developing countries and remote areas.[1–3] Interfacial solar steam generation[4–34] has demonstrated great potential in various fields such as desalination,[4–7] waste-water treatment,[8,9] and electricity generation.[10] In previous studies, high energy-transfer efficiency from solar to steam has been demonstrated through rational designs of material structures,[8,11] photon management,[5,12] heat localization,[13] and water supply.[4,9] In most if not all of the previous studies of interfacial solar steam generation, the internal enthalpy of steam is usually lost to the environment as steam condenses to form water (Figure 1A). Recently, Zhou's group demonstrated the concept of simultaneous generations of steam and electricity (~1 W/m^2 under one-sun illumination, ~0.1% efficiency) by taking advantage of the evaporation-induced salinity gradient.[10] A significant increase in power generation is expected to open up tremendous opportunities. In this work, by storing and recycling the internal enthalpy of steam during steam condensation, we demonstrate simultaneous generation of clean water (72.2% efficiency) and electricity (~1.23% efficiency) with solar energy as the only energy input (Figure 1B). In addition, the integrated capability of thermal storage enables the generation of electricity over an extended period after the light is extinguished, as illustrated in more detail below.

RESULTS AND DISCUSSION

The storage and recycling of interfacial solar steam enthalpy for simultaneous generation of clean water and electricity is shown in Figure 1B (the real setup is shown in Figure S1). This high-temperature steam generated by an interfacial solar steam generator (as shown in Figure S1A) flows into the area of thermal storage and water generation, with an aluminum chamber wrapped by a polyurethane foam (as shown

Context & Scale

Interfacial solar steam generation has recently demonstrated great potential in various applications, from desalination and distillation to catalysis. However, in most previous studies the steam enthalpy was typically lost to the environment during condensation without any utilization. In this work, we demonstrate that through designs and integrations of materials and systems, steam enthalpy can be stored and recycled for power generation (at efficiency of 1.23%), in addition to 72.2% solar-to-vapor efficiency. In addition, the integrated capability of thermal storage can enable electricity generation over an extended period after the light source is turned off. Combining solar energy conversion, storage, and utilization, this method based on low cost and scalable graphite/nonwoven films provides a complementary system to produce clean water and electricity, the basic needs in various resource-constrained areas.

Please cite this article in press as: Li et al., Storage and Recycling of Interfacial Solar Steam Enthalpy, Joule (2018), https://doi.org/10.1016/j.joule.2018.08.008

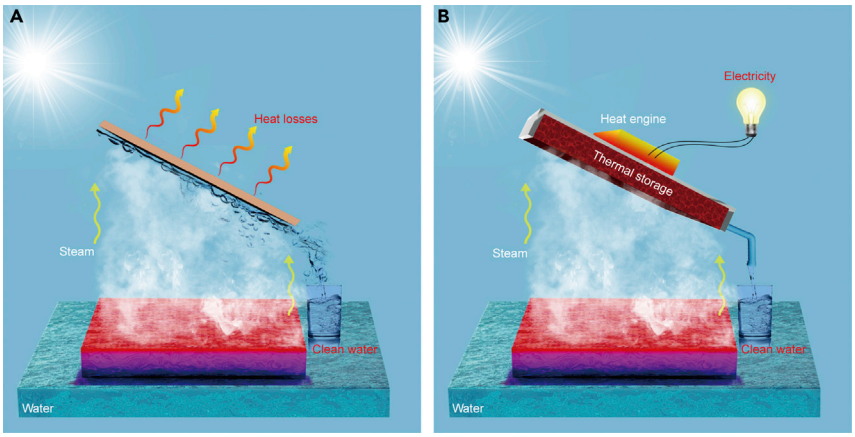

Figure 1. Schematic of the Condensation Processes of Interfacial Solar Steam Generation
(A) Traditionally, steam condenses to form water with enthalpy lost to the environment.
(B) Storage and recycling of interfacial solar steam enthalpy for simultaneous generation of clean water and electricity.

in Figure S1B) for thermal insulation. Because of the heat exchange between high-temperature steam and the chamber, steam will be condensed to produce clean water at the outlet of the chamber, while the energy in the steam is reserved in the chamber to maintain it at a high temperature. The temperature gradient formed between this chamber and the room-temperature environment can then be used for electricity generation by using the thermoelectric modules (based on Bi_2Te_3 materials; for more details see Experimental Procedures).

The device performance depends on the properties of the solar absorber. Currently there are mainly two categories of nanomaterials for solar steam generation, namely carbon-based and plasmonic-based absorbers. Here, graphite/nonwoven film is selected as a solar absorber of interfacial solar steam generation mainly because it has efficient absorption, excellent stability and foldability, and can be fabricated through a scalable and cost-effective process. All of these features are detailed below. The graphite/nonwoven absorber can be conveniently fabricated by spraying the ethanol solution of graphite toward a piece of preheated nonwoven material (for more details see Experimental Procedures); corresponding optical images of nonwoven fabric (10 cm × 5 cm) before and after spray-coating are shown in Figures 2A and 2C. The corresponding scanning electron microscopy (SEM) images are shown in Figures 2B and 2D, which demonstrate clearly the graphite particles (size about a few hundred nanometers) on nonwoven fibers. This graphite/nonwoven film has efficient and broadband absorption, with about 98% weighted absorption (by standard AM 1.5G solar spectrum) from 250 nm to 2,500 nm (Figure 2E). Another unique property of this graphite/nonwoven film is that it can maintain its integrity when immersed in water and even after shaking for a long time (Figures 2F and 2G), which is beneficial for practical applications. Moreover, the absorber can be easily folded because of the flexible nonwoven substrates (as shown in Figure S2), advantageous for large-scale carriage and deployment.

The mass change over time under different solar concentrations is shown in Figure 3A. In the beginning, the mass change is not obvious within first few minutes (for example, 2 min under illumination of 30 kW/m^2) because of the initial inner condensation of steam in the solar steam-generation device. Thereafter it starts to

[1]National Laboratory of Solid State Microstructures, College of Engineering and Applied Sciences, School of Physics, Key Laboratory of Intelligent Optical Sensing and Integration, and Collaborative Innovation Center of Advanced Microstructures, Nanjing University, Nanjing 210093, P.R. China

[2]These authors contributed equally

[3]Lead Contact

*Correspondence: jiazhu@nju.edu.cn

https://doi.org/10.1016/j.joule.2018.08.008

Please cite this article in press as: Li et al., Storage and Recycling of Interfacial Solar Steam Enthalpy, Joule (2018), https://doi.org/10.1016/j.joule.2018.08.008

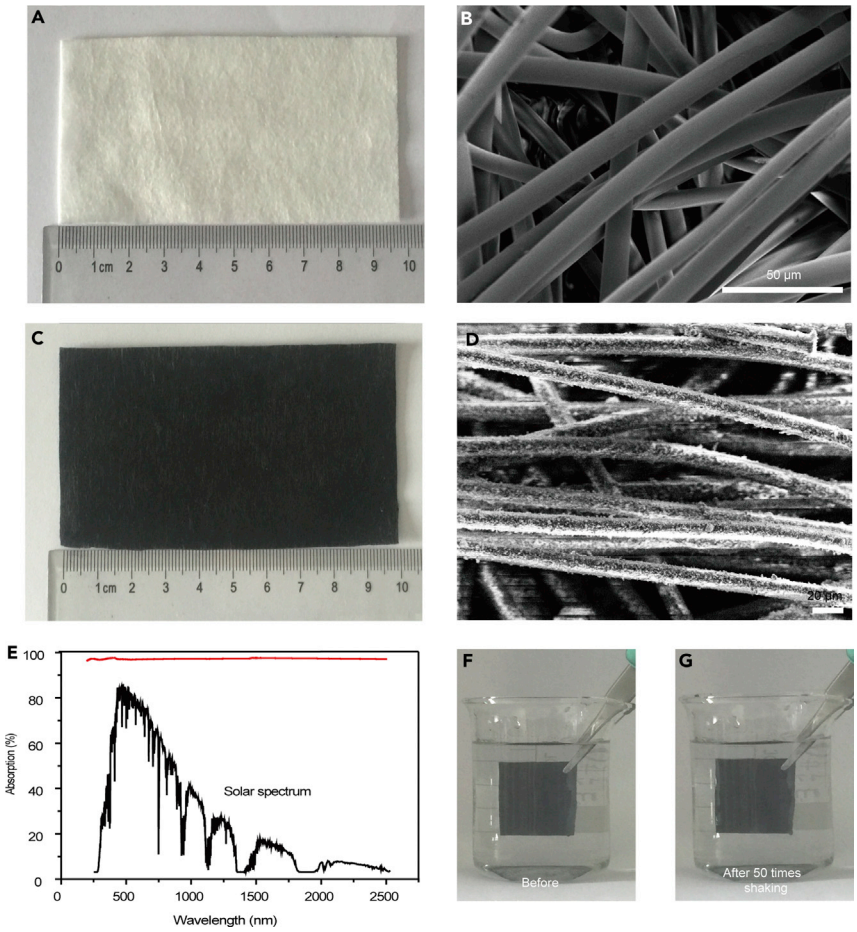

Figure 2. Solar Absorbers Based on Graphite/Nonwoven

(A and B) Optical image (A) and SEM image (B) of nonwoven material.

(C and D) Optical image (C) and SEM image (D) of graphite/nonwoven.

(E) Absorption spectrum of graphite/nonwoven from 250 to 2,500 nm.

(F) Optical image of graphite/nonwoven in water.

(G) Optical image of graphite/nonwoven in water after shaking 50 times.

show the nearly linear mass change over time under 30 kW/m^2, which is orders of magnitude shorter than that of the traditional bulk water heating (around 20 min, see Figure S3). That is a direct indication of much reduced heat loss for interfacial heating and therefore reduced time to reach a steady state. As shown in Figure 3B, the temperature of steam can reach a steady state after 666 s, 146 s, 40 s, and 32 s under 8, 17, 22, and 30 kW/m^2, respectively, which is also an indication of reduced time response of interfacial heating. The formula $\eta = mh_{LV}/P_{in}$ is used for calculating the solar-to-steam efficiency (η), where m is the mass flux, h_{LV} is total liquid-vapor phase-change enthalpy (phase-change enthalpy + sensible heat), and P_{in} is the received power density of the solar irradiation on the absorber surface.[13] As shown in Figure 3C, the evaporation rates (obtained from the slope of the mass change curves at steady state) are 4.2, 15.5, 24.3, and 34.8 kg/m^2 h under 8, 17, 22, and 30 kW/m^2, respectively, and corresponding efficiencies are 36.4%, 64.7%, 73.3%, and 81.7%, respectively. It should be noted that this efficiency is achieved in a semi-closed system that is different from earlier reported efficiency in an open system (for more details see Supplemental Note 1). This increased trend of efficiency

Please cite this article in press as: Li et al., Storage and Recycling of Interfacial Solar Steam Enthalpy, Joule (2018), https://doi.org/10.1016/j.joule.2018.08.008

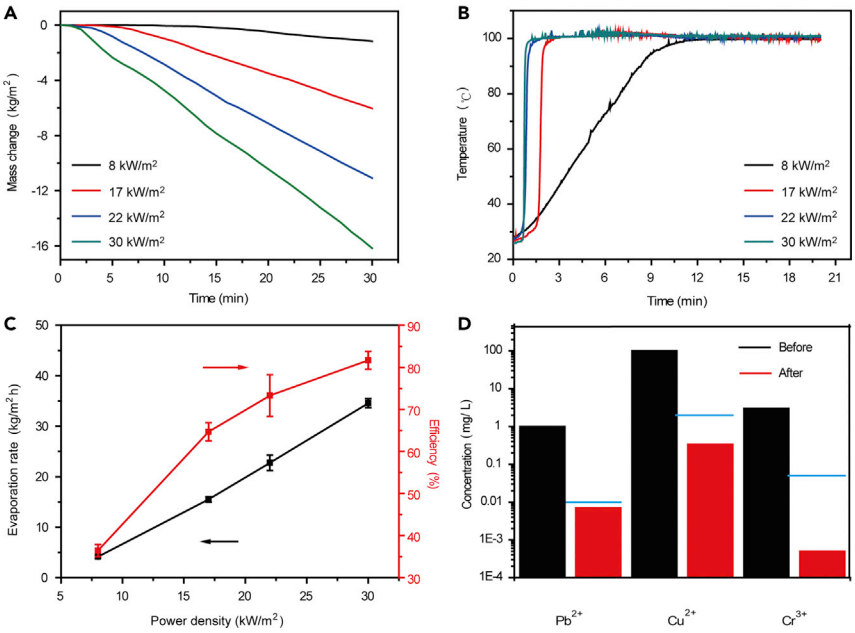

Figure 3. Interfacial Solar Steam Generation

(A) Mass change over time of interfacial solar steam generator under different solar irradiations.

(B) Temperature of output steam over time under different solar irradiations.

(C) Dependence of evaporation rate and corresponding efficiency on optical concentrations. Error bars indicate the SD of the measurements.

(D) Concentrations of various metal ions before and after treatment (the blue line refers to the WHO standards for drinking water).

with increased power input is consistent with previous studies,[5,13] and can be ascribed to the decreasing ratio of heat loss under higher illumination (for more details about thermal analysis see Supplemental Note 2). As shown in Figure S4, the evaporation rates with integrated thermal storage are 3.0, 14.5, 21.7, and 31.6 kg/m^2 h under 8, 17, 22, and 30 kW/m^2, respectively, with corresponding efficiencies of 26.5%, 60.5%, 70.0%, and 74.7%, respectively. The clean water can be collected once the steam is condensed, even directly from contaminated water sources. As an example of demonstration, water contaminated with rich Pb^{2+}, Cu^{2+}, and Cr^{3+} ions, common heavy metal pollutants, is used. As shown in Figure 3D, the result shows that the output water (the Pb^{2+}, Cu^{2+}, and Cr^{3+} ion concentration 0.007, 0.338, and 5×10^{-4} mg/L, respectively) can reduce the metal ion concentrations by two orders of magnitude, and meet the World Health Organization (WHO) drinking water standard (Pb^{2+}: 0.01 mg/L; Cu^{2+}: 2 mg/L; Cr^{3+}: 0.05 mg/L).[35]

With the chamber temperature of the thermal storage area maintained at 100°C and room temperature (25°C), the thermoelectric module can be used for electricity generation. The output of the thermoelectric module is highly dependent on the temperature difference on its two sides. Once the light source is turned on, both the open-circuit voltage and short-circuit current will first increase as the chamber temperature increases until reaching the steady state at around 100°C, as shown in Figures 4A and 4B (corresponding temperatures of hot side and cool side are shown in Figure S5). With the increased solar power illumination, a larger amount of steam will be generated to transfer more condensation latent heat to the thermoelectric module, therefore further enhancing the open-circuit voltage and short-circuit current, up to 3.87 V and 0.55 A under 30 kW/m^2.

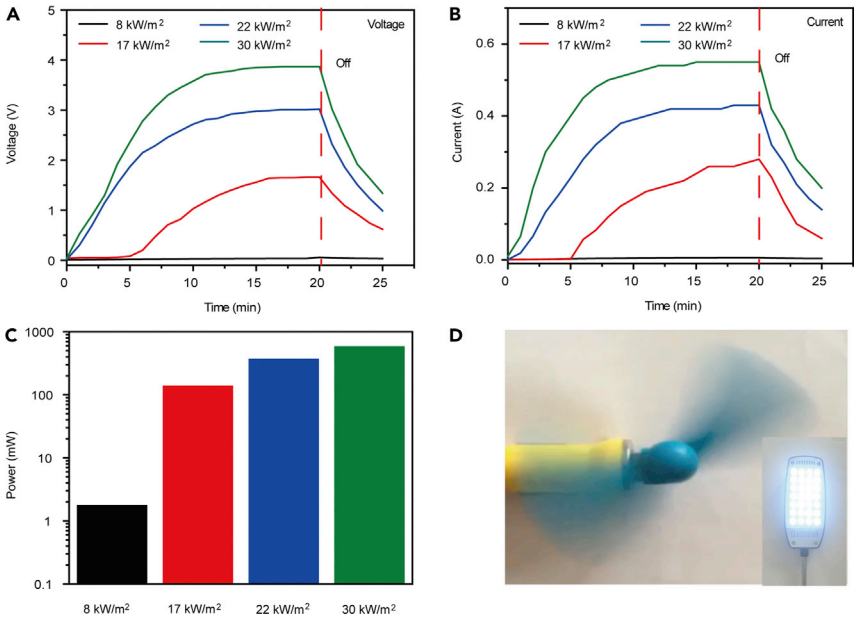

Figure 4. Performance of Electricity Generation

(A) Open-circuit voltage over time under different solar irradiations.

(B) Short-circuit current over time under different solar irradiations.

(C) Maximum output power of the thermoelectric device under different solar irradiations.

(D) Optical image of an operating electric fan and an illuminating light-emitting diode powered by interfacial solar steam generation. A movie showing simultaneous generations of electricity and clean water is provided in Video S1.

Figure 4C shows the output power of the thermoelectric device under different solar irradiations. We found that the maximum output power was achieved when external resistance is about 6 Ω and output power is 1.7, 135.7, 363.0, and 574 mW under 8, 17, 22, and 30 kW/m^2, respectively, with corresponding output power density of 0.9, 69.2, 185.2, and 292.9 W/m^2, respectively. The formula $\eta = P_e/P_{in}$ is used for calculating the power generation efficiency (η), where P_e and P_{in} are the output energy of power generation and input energy of solar. It can be seen that the maximum efficiency can reach 0.98% under 30 kW/m^2 (energy analysis is detailed in Supplemental Note 2). The efficiency can be further enhanced by increasing the steam temperature using techniques such as superheated steam (for more details see Supplemental Note 3). It can be seen that the open-circuit voltage and short-circuit current can reach to 4.15 V and 0.61 A, while the maximum efficiency can reach 1.23% under 30 kW/m^2 (comparison with solar cell-based technology is detailed in Supplemental Note 4). Therefore various applications can be supported, such as continuous operation of an electric fan (1 W) and 28 light-emitting diodes (total power 1.5 W), as shown in Figure 4D. Given advanced thermal management to further increase the steam temperature and exciting progress in the field of thermoelectrics and solar desalination, it is expected that the performance of this system can be further improved (more analysis is provided in Supplemental Note 5).

In addition to simultaneous generation of purified water and electricity, another unique feature of this device is that it has integrated thermal storage, which can enable power generation over an extended period without sunlight. After the light source is turned off, the polyurethane foam-wrapped aluminum chamber with thermal capacity will release sensible heat to maintain electricity generation, as shown in Figures 4A and 4B (for a movie of continuous generation of electricity without

Please cite this article in press as: Li et al., Storage and Recycling of Interfacial Solar Steam Enthalpy, Joule (2018), https://doi.org/10.1016/j.joule.2018.08.008

sunlight, see Video S2). The duration of the extended period can be tuned by thermal capacity or mass of chapter materials (for more analysis see Supplemental Note 6), which can be used to reduce the influence of intermittent illumination such as rolling cloud cover (for more details see Supplemental Note 7). The performance is expected to be further promoted by employing phase-change materials that can tune the mismatch between solar illumination and power usage.

Conclusions

This work shows that by storing and recycling steam enthalpy derived from the solar steam process, we can enable simultaneous generation of clean water and electricity. The results showed that the energy-transfer efficiency of solar to steam can reach 72.2% with extra electricity power (with 1.23% efficiency) generated simultaneously (a comparison with solar cell-based technology is provided in Supplemental Information). With advanced thermal management to further elevate the working temperature and exciting progress in the field of thermoelectrics and solar desalination, it is expected that the performance of this system can be further improved (for more analysis see Supplemental Information). This approach with scalable materials and processes, high energy-transfer efficiency, and integrated storage capability will provide an attractive avenue through which to produce electricity and clean water in an individualized manner, particularly desirable in various off-grid areas.

EXPERIMENTAL PROCEDURES

Fabrication of Solar Absorbers (Graphite/Nonwoven Film)

Graphite particles with diameter of about 30 nm were dispersed in ethanol solution at the concentration of 5 mg/mL followed by 2 hr of ultrasonication. The graphite solution was then sprayed through a commercial airbrush (nozzle diameter 0.3 mm; Ustar CD-601, Taiwan) toward the preheated nonwoven to produce graphite/nonwoven film.

Interfacial Solar Steam-Generation Device

Hydrophilic nonwoven-wrapped polystyrene foam (about 2 cm thick, as water supply layer and thermal insulation layer) was floated on the surface solution in a beaker with an insulation layer. A graphite/nonwoven film was placed on the surface of nonwoven-wrapped polystyrene foam. A transparent quartz plate covered the upper surface of the beaker while a thermal insulated tube was connected inside the beaker.

Electricity Generation Setup

As shown in Figure S1, the commercial thermoelectric module (Bi_2Te_3, length 8 cm, width 4 cm, height 3.4 mm, ZT about 1 at ~373 K) was selected as the power generation device. The cool side was connected to a cooling fin placed in water and the hot side was connected to a two-end open insulation chamber.

Characterizations

The morphologies and structures of the solar absorber (graphite/nonwoven) were characterized by a scanning electron microscope (Dual-beam FIB 235; FEI Strata). The absorption of graphite/nonwoven was measured from 200- to 2,500-nm wavelength using a UV-visible spectroscope (UV-3600; Shimadzu). The concentration of heavy metal ions was characterized by ICP-OES (0.1 mg/L accuracy, PTIMA 5,300 DV; PerkinElmer Instruments).

Simultaneous Generations of Electricity and Clean Water

The device was irradiated by a xenon lamp (HSX-F300; Excelitas). The temperature of the steam was recorded by thermocouples (placed in insulated tube, as shown in Figure S1A, T_1). The temperature of the hot side of the thermoelectric module was recorded by thermocouples (placed in an aluminum chamber, as shown in Figure S1B, T_2 and T_3). The mass change was monitored by electronic analytical scale, recorded in real time by the computer (with RS-232 serial ports) and used to determine the mass change of solar steam generation. The open-circuit voltage and short-circuit current was recorded by a multimeter. The power line was obtained by changing the external resistance.

SUPPLEMENTAL INFORMATION

Supplemental Information includes Supplemental Experimental Procedures, 11 figures, and 2 videos and can be found with this article online at https://doi.org/10.1016/j.joule.2018.08.008.

ACKNOWLEDGMENTS

We acknowledge the micro-fabrication center of the National Laboratory of Solid State Microstructures for technical support. This work is jointly supported by the National Key Research and Development Program of China (no. 2017YFA0205700) and the State Key Program for Basic Research of China (no. 2015CB659300), National Natural Science Foundation of China (nos. 11621091, 11574143, 61735008), and the Fundamental Research Funds for the Central Universities (nos. 021314380135, 021314380128).

AUTHOR CONTRIBUTIONS

J.Z., X.L., and X.M. designed research; X.L. and X.M. performed research; J.L., N.X., P.Z., and B.Z. contributed new reagents/analytical tools; X.L., X.M., S.Z., and J.Z. analyzed data; X.L., X.M., and J.Z. wrote the paper.

DECLARATION OF INTERESTS

The authors declare no competing interests.

Received: November 22, 2017
Revised: April 17, 2018
Accepted: August 17, 2018
Published: September 7, 2018

REFERENCES

1. Mekonnen, M., and Hoekstra, A. (2016). Four billion people facing severe water scarcity. Sci. Adv. *2*, e1500323.

2. Schewea, J., Heinke, J., Gerten, D., Haddeland, I., Arnell, N., Clark, D., Dankers, R., Eisner, S., Fekete, B., et al. (2014). Multimodel assessment of water scarcity under climate change. Proc. Natl. Acad. Sci. USA *111*, 3245–3250.

3. Mcilvaine, R. (2014). A new approach for evaluating energy choices. Electric. J. *27*, 72–79.

4. Li, X., Xu, W., Tang, M., Zhou, L., Zhu, B., Zhu, S., and Zhu, J. (2016). Graphene oxide-based efficient and scalable solar desalination under one sun with a confined 2D water path. Proc. Natl. Acad. Sci. USA *113*, 13953–13958.

5. Zhou, L., Tan, Y., Wang, J., Xu, J., Yuan, Y., Cai, W., Zhu, S., and Zhu, J. (2016). 3D self-assembly of aluminium nanoparticles for plasmon-enhanced solar desalination. Nat. Photonics *10*, 393–398.

6. Yang, Y., Zhao, R., Zhang, T., Zhao, K., Xiao, P., Ma, Y., Shi, G., and Chen, Y. (2018). Graphene-based standalone solar energy converter for water desalination and purification. ACS Nano *12*, 829–835.

7. Wang, X., Ou, G., Wang, N., and Wu, H. (2016). Graphene-based recyclable photo-absorbers for high-efficiency seawater desalination. ACS Appl. Mater. Interfaces *8*, 9194–9199.

8. Ren, H., Tang, M., Guan, B., Wang, K., Yang, J., Wang, F., Wang, M., Shan, J., Chen, Z., Wei, D., et al. (2017). Hierarchical graphene foam for efficient omnidirectional solar-thermal energy conversion. Adv. Mater. *29*, 1702590.

9. Li, X., Lin, R., Ni, G., Xu, N., Hu, X., Zhu, B., Lv, G., Li, J., Zhu, S., and Zhu, J. (2018). Three-dimensional artificial transpiration for efficient solar waste-water treatment. Nat. Sci. Rev. *5*, 70–77.

10. Yang, P., Liu, K., Chen, Q., Li, J., Duan, J., Xue, G., Xu, Z., Xie, W., and Zhou, J. (2017). Solar-driven simultaneous steam production and electricity generation from salinity. Energy Environ. Sci. *10*, 1923–1927.

11. Chen, C., Li, Y., Song, J., Yang, Z., Kuang, Y., Hitz, E., Jia, C., Gong, A., Jiang, F., Zhu, J.Y., et al. (2017). Highly flexible and efficient solar

steam generation device. Adv. Mater. *29*, 1701756.

12. Neumann, O., Feronti, C., Neumann, A.D., Dong, A., Schell, K., Lu, B., Kim, E., Quinn, M., Thompson, S., Grady, N., et al. (2013). Compact solar autoclave based on steam generation using broadband light-harvesting nanoparticles. Proc. Natl. Acad. Sci. USA *110*, 11677–11681.

13. Ghasemi, H., Ni, G., Marconnet, A.M., Loomis, J., Yerci, S., Miljkovic, N., and Chen, G. (2014). Solar steam generation by heat localization. Nat. Commun. *5*, 4449.

14. Shi, F., Li, R., Jin, Y., Zhuo, S., Shi, L., Chang, J., Hong, S., Ng, K., and Wang, P. (2018). A 3D photothermal structure toward improved energy efficiency in solar steam generation. Joule *2*, 1171–1186.

15. Jia, C., Li, Y., Yang, Z., Chen, G., Yao, Y., Jiang, F., Kuang, Y., Pastel, G., Xie, H., Gao, T., et al. (2017). Rich mesostructures derived from natural woods for solar steam generation. Joule *1*, 588–599.

16. Li, X., Li, J., Lu, J., Xu, N., Chen, C., Min, X., Zhu, B., Li, H., Zhou, L., Zhu, S., et al. (2018). Enhancement of interfacial solar vapor generation by environmental energy. Joule *2*, 1331–1338.

17. Li, Y., Gao, T., Yang, Z., Chen, C., Luo, W., Song, J., Hitz, E., Jia, C., Zhou, Y., Liu, B., et al. (2017). 3D-printed, all-in-one evaporator for high-efficiency solar steam generation under 1 sun illumination. Adv. Mater. *29*, 1700981.

18. Gao, X., Ren, H., Zhou, J., Du, R., Yin, C., Liu, R., Peng, H., Tong, L., Liu, Z., and Zhang, J. (2017). Synthesis of hierarchical graphdiyne-based architecture for efficient solar steam generation. Chem. Mater. *29*, 5777–5790.

19. Zhuang, S., Zhou, L., Xu, W., Xu, N., Hu, X., Li, X., Lv, G., Zheng, Q., Zhu, S., Wang, Z., and Zhu, J. (2017). Tuning transpiration by interfacial solar absorber-leaf engineering. Adv. Sci. (Weinh) *5*, 1700497.

20. Sajadi, S.M., Farokhnia, N., Irajizad, P., Hasnain, M., and Ghasemi, H. (2016). Flexible artificially-networked structure for ambient/high pressure solar steam generation. J. Mater. Chem. A *4*, 4700–4710.

21. Zhang, L., Tang, B., Wu, J., Li, R., and Wang, P. (2015). Hydrophobic light-to-heat conversion membranes with self-healing ability for interfacial solar heating. Adv. Mater. *27*, 4889–4909.

22. Jiang, Q., Tian, L., Liu, K.K., Tadepalli, S., Raliya, R., Biswas, P., Naik, R.R., and Singamaneni, S. (2016). Bilayered biofoam for highly efficient solar steam generation. Adv. Mater. *28*, 9400–9407.

23. Ni, G., Li, G., Boriskina, S.V., Li, H., Yang, W., Zhang, T., and Chen, G. (2016). Steam generation under one sun enabled by a floating structure with thermal concentration. Nat. Energy *1*, 16126–16132.

24. Mu, C., Song, Y., Deng, K., Lin, S., Bi, Y., Scarpa, F., and Crouse, D. (2017). High solar desalination efficiency achieved with 3D Cu_2ZnSnS_4 nanosheet-assembled membranes. Adv. Sustain. Syst. *1*, 1700064.

25. Zhang, P., Li, J., Lv, L., Zhao, Y., and Qu, L. (2017). Vertically aligned graphene sheets membrane for highly efficient solar thermal generation of clean water. ACS Nano *11*, 5087–5093.

26. Zhang, L., Xing, J., Wen, X., Chai, J., Wang, S., and Xiong, Q. (2017). Plasmonic heating from indium nanoparticles on a floating microporous membrane for enhanced solar seawater desalination. Nanoscale *9*, 12843–12849.

27. Wang, G., Fu, Y., Guo, A., Mei, T., Wang, J., Li, J., and Wang, X. (2017). Reduced graphene oxide-polyurethane nanocomposite foams as a reusable photo-receiver for efficient solar steam generation. Chem. Mater. *29*, 5629–5636.

28. Gao, M., Connor, P., and Ho, G. (2016). Plasmonic photothermic directed broadband sunlight harnessing for seawater catalysis and desalination. Energy Environ. Sci. *9*, 3151–3160.

29. Liu, C., Huang, J., Hsiung, C.E., Tian, Y., Wang, J., Han, Y., and Fratalocchi, A. (2017). High-performance large-scale solar steam generation with nanolayers of reusable biomimetic nanoparticles. Adv. Sustain. Syst. *1*, 1600013.

30. Xu, N., Hu, X., Xu, W., Li, X., Zhou, L., Zhu, S., and Zhu, J. (2017). Mushrooms as efficient solar steam-generation devices. Adv. Mater. *29*, 1606762.

31. Li, R., Zhang, L., Shi, L., and Wang, P. (2017). MXene Ti_3C_2: an effective 2D light-to-heat conversion material. ACS Nano *11*, 3752–3759.

32. Zhao, F., Zhou, X., Shi, Y., Qian, X., Alexander, M., Zhao, X., Mendez, S., Yang, R., Qu, L., and Yu, G. (2018). Highly efficient solar vapour generation via hierarchically nanostructured gels. Nat. Nanotechnol. https://doi.org/10.1038/s41565-018-0097-z.

33. Xu, W., Hu, X., Zhuang, S., Wang, Y., Li, X., Zhou, L., Zhu, S., and Zhu, J. (2018). Flexible and salt resistant janus absorbers by electrospinning for stable and efficient solar desalination. Adv. Energy Mater. *8*, 1702884.

34. Zhou, M., and Yu, Z. (2018). Artificial transpiration: an efficient means of waste-water-treatment. Nat. Sci. Rev. *5*, 121–122.

35. World Health Organization. (2011). Safe Drinking Water from Desalination (WHO). http://who.int/water_sanitation_health/publications/2011/desalination_guidance/en/.